

2. TEXTURAL AND MINERALOGIC VARIATIONS IN GABBROIC ROCKS FROM HOLE 735B¹

S. H. Bloomer,² P. S. Meyer,^{3,4} H.J.B. Dick,³ K. Ozawa,⁵ and J. H. Natland⁶

ABSTRACT

Gabbroic rocks from Hole 735B span a complete range of tholeiitic differentiates from troctolites to olivine gabbros, to gabbro-norites, to oxide-rich, olivine-bearing gabbros. The olivine gabbros (66% of the core) have homogeneous compositions (Fo 77 ± 2 , clinopyroxene Mg/Mg+Fe 0.84 ± 0.01 , An 60 ± 1). The modes, grain-size variations, and textures of the olivine gabbro indicate that they formed by *in-situ* crystallization. Sharp lithologic transitions from olivine gabbro to oxide-bearing gabbro (An 36 to 44, Fo 43 to 58, clinopyroxene Mg/Mg+Fe 0.65 to 0.72) reflect intrusion of the latter into the former. These intrusive relationships are manifest by re-equilibration of mafic phases in the olivine gabbro adjacent to contacts and inclusion of olivine gabbros in oxide-bearing gabbro. Intrusion of the oxide gabbros was localized along deformation zones in the near-rigid olivine gabbros. Rapid changes in grain size in olivine and oxide-bearing gabbros do not correspond to compositional offsets. These textural changes most likely reflect localized changes in nucleation and growth rates. Locally, intrusive relationships between microgabbros and gabbros, and mixed microgabbros and gabbros, may be the result of crystal-rich slumps and plumes developed along the margins of an irregularly shaped magma chamber. The olivine gabbros and oxide-bearing gabbros may have formed from a single intrusion. The troctolites in the lowermost sections of the hole (An 68, Fo 81, clinopyroxene Mg/Mg+Fe 0.87) are intrusive into the section and mark the margins of a second intrusion.

INTRODUCTION

Most of our models of mid-ocean ridge magmatic processes have been derived from geophysical surveys and petrologic and geochemical studies of fresh, basaltic rocks. However, gabbroic rocks from the mid-ocean ridges offer a different perspective of magmatic processes at spreading ridges. Plutonic rocks have been recovered in numerous localities (e.g., Fox and Stroup, 1981; Engel and Fisher, 1975; Fisher et al., 1986; Miyashiro and Shido, 1980; Tiezzi and Scott, 1980; Walker and DeLong, 1984; Batiza and Vanko, 1985; Hebert et al., 1983; Elthon, 1987). Dredged gabbroic samples have been used to examine gabbro-basalt relationships (Tiezzi and Scott, 1980; Bloomer et al., 1989), conditions of crystallization (Elthon, 1987), compositions and diversity of parental melts (Bloomer et al., 1989), and the dynamics of crystallization of plutonic rocks (Bloomer et al., 1989; Meyer et al., 1989). Interactions of magma and cumulates may be an important process contributing to the diversity of trace-element signatures in erupted basalts (Langmuir, 1989). Our efforts to understand the development of magma chambers at mid-ocean ridges have been hindered by the lack of stratigraphically well-located plutonic samples and the inherent difficulties in working on cumulus-textured rocks.

The 436 m of gabbro recovered from Hole 735B has provided us with a unique opportunity to examine the development of a portion of layer 3 at a slowly spreading ridge crest. Understanding the evolution of this crust requires an examination of the structural, petrographic, petrologic, and

mineralogic characteristics of the various gabbros. This study presents a summary of data on the textural and mineralogic characteristics of the principal igneous rock types in the Site 735B gabbros.

BACKGROUND

Site 735B was drilled on a shallow (731 m) transverse ridge on the eastern side of the Atlantis II Fracture Zone (Fig. 1), between magnetic anomalies 5 and 5a approximately 93 km south of the present-day axis of the Southwest Indian Ridge (Dick et al., this volume). The hole is 500.7 m deep and 436 m of gabbroic rocks was recovered. The site lies in crust formed about 11 Ma (Dick et al., this volume), and the platform is about 18 km from the active deformation zone of the transform fault. At the time this piece of crust formed, the Southwest Indian Ridge was spreading at a full rate of 0.8 to 1.2 cm/yr (Fisher and Sclater, 1983), which is at the low end of the spectrum for mid-ocean ridges. Such low spreading rates imply extremely low rates of crustal accretion and magma supply.

Macroscopic examination of the 735B cores on board the *JOIDES Resolution* (Robinson, Von Herzen, et al., 1989) and subsequent re-description of the core at the Gulf Coast Repository at Texas A&M University (Dick et al., this volume) identified nine primary igneous lithologies: troctolite, troctolitic microgabbro, olivine gabbro, gabbro-norite, microgabbro-norite, disseminated oxide olivine gabbro, oxide olivine gabbro, trondhjemite, and basalt, with gradations between some of the lithologies. The nomenclature follows the recommended IUGS classification scheme (Streckeisen, 1976), with minor modifications: oxide olivine gabbros are olivine gabbros having greater than 5% iron-titanium oxides, while disseminated oxide olivine gabbros contain less than 2% iron-titanium oxides, as well as orthopyroxene and/or inverted pigeonite. As will be shown here, mineral compositions in these rock types are distinctly different. The term microgabbro is used for fine-grained equivalents, those having less than a 1-mm average grain size—hence troctolitic microgabbro and microgabbro-norite. Nearly 95% of the core is made up of olivine

¹ Von Herzen, R. P., Robinson, P. T., et al., 1991. *Proc. ODP, Sci. Results*, 118: College Station, TX U.S.A. (Ocean Drilling Program).

² Department of Geology, Boston University, Boston MA 02215.

³ Department of Geology and Geophysics, Woods Hole Oceanographic Institution, Woods Hole, MA 02543.

⁴ Department of Physical Science, Rhode Island College, Providence, RI 02908.

⁵ Faculty of Science, University of Tokyo, Tokyo, Japan.

⁶ Geological Research Division, Scripps Institution of Oceanography, La Jolla, CA 92093.

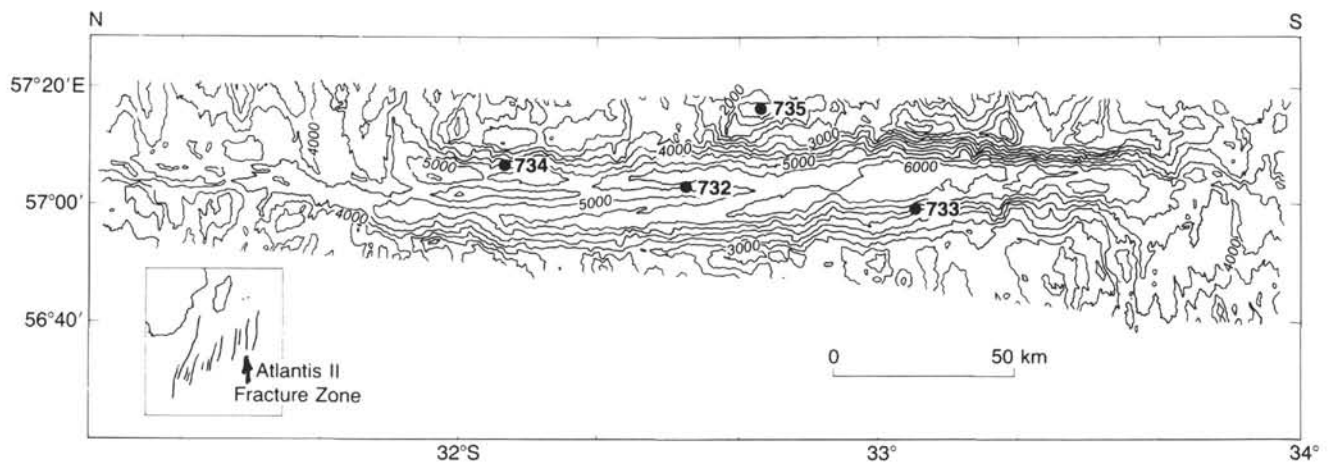


Figure 1. Bathymetric map at 500-m contour intervals of the Atlantis II Fracture Zone, Southwest Indian Ridge, showing Leg 118 drill sites. Survey from *Conrad* cruise 27-09, 1986 (H. Dick, Chief Scientist, with D. Gallo and R. Tyce).

gabbros (66%), oxide olivine gabbros (15%), disseminated oxide olivine gabbros (8%), and gabbronorites (5.5%).

The core was divided into six units and twelve subunits based upon the principal igneous lithologies (Tables 1 and 2). These units are listed in Table 1; a schematic section of the core with downcore olivine compositional variations is shown in Figure 2. Subunit IA and Units IV and V are lithologically homogeneous and comprise gabbronorite, oxide olivine gabbro, and olivine gabbro, respectively. Unit V is relatively undeformed; subunit IA is highly deformed and has porphyroclastic to mylonitic textures.

The other units (IB, II, III, and VI) are composites in which olivine gabbros and microgabbros are intruded by olivine-oxide gabbros, disseminated oxide olivine gabbros, and in Unit VI, troctolites and troctolitic gabbros. The olivine microgabbros and troctolitic microgabbros occur as both discrete intrusions into olivine gabbro and as pods or segregations within the olivine gabbro (Dick et al., this volume). The oxide-bearing gabbros occur as thin, millimeter- and centimeter-wide veins and as layers or seams several meters thick. The thinnest veins are nearly monomineralic, with oxides bordered by pyroxene-rich reaction zones. The oxide-rich zones are highly deformed and, in fact, are concentrated along loci of deformation within the olivine gabbros (Dick et al., this volume). The deformation textures in many of the oxide gabbros include a hypersolidus magmatic foliation and a superimposed subsolidus brittle-ductile deformation.

Detailed lithostratigraphy, both igneous and metamorphic, is presented in Dick et al. (this volume).

METHODS

Polished thin sections were described for samples from homogenous intervals of most rock types within each subunit, as well as from contacts and size- or phase-layered intervals. Representative slides were selected for electron probe analysis. The sampling is fairly representative of the core at about a 5-m interval (about 100 samples in 500 m), though the upper parts of Units I and IB may be underrepresented because of the extreme deformation in those parts of the core.

Most mineral analyses were performed on the JEOL 733 Superprobe at MIT using a modified Bence-Albee reduction scheme. A focused (1 to 2 μ spot), 10 nA beam was used for all analyses. Standardization was performed using a combination

of natural and synthetic standards. Some samples were analyzed on the JEOL 733 Superprobe at the Harvard-Smithsonian Astrophysical Observatory in Cambridge (with the same conditions as at the MIT probe, excepting a 20 nA beam current). Analyses of adjacent points in the same samples showed the numbers from the two microprobes to agree to better than 2%, except in the case of Na_2O for plagioclase. The Smithsonian probe did not use a high-Na plagioclase standard and gave consistently high corrected Na_2O values (approximately 2.2 mol% An for the range of plagioclase compositions measured on the Smithsonian probe). Plagioclase compositions reported here have been corrected to values from the MIT instrument. Average core compositions for lithologies within each unit are presented in Table 3.

Table 1. Summary of primary igneous stratigraphy in Hole 735B after Dick et al. (this volume).

Lithologic unit	Depth top (m)	Depth bottom (m)	Lithologies
IA	0	7-1, 114 (Pc. 14)	Massive gabbronorite
IIB	27.99	10-1, 70 (Pc. 12)	Olivine gabbro and gabbronorite
II	37.47	35-6, 72 (Pc. 7)	Mixed olivine gabbro/microgabbro and oxide gabbro
IIIA	170.22	37-3, 70 (Pc. 3)	Olivine gabbro and disseminated oxide olivine gabbro
IIIB	180.09	43-3, 98 (Pc. 11)	Massive disseminated oxide olivine gabbro
IIIC	209.45	46-2, 150 (Pc. 7c)	Disseminated oxide olivine gabbro, olivine gabbro and olivine-oxide gabbro
IV	223.57	56.3, 116 (Pc. 29)	Massive olivine oxide gabbro
V	274.06	74-6, 3 (Pc. 1)	Massive olivine gabbro
VIA	382.40	77-1, 55 (Pc. 2e)	Olivine gabbro/microgabbro, oxide microgabbronorite, oxide-olivine gabbro
VIB	404.01	79-4, 56 (Pc. 2f)	Olivine gabbro/microgabbro, oxide-olivine gabbro, disseminated oxide olivine gabbro
VIC	419.28	81-1, 26 (Pc. 1b)	Olivine gabbro, troctolite, oxide olivine gabbro
VID	433.77	88-1, 70 (Pc. 2)	Olivine gabbro, olivine oxide gabbro, troctolite, troctolitic gabbro

Table 2. Percentages of principal rock types from Hole 735B (by unit).

Lithologic unit: Thickness (m):	I	IB	II	IIIA	IIIB	IIIC	IV	V	VIA	VIB	VIC	VID	TOTAL
27.99	9.48	132.75	9.87	29.36	14.12	50.49	108.34	21.61	15.27	14.49	66.70	500.7	
Rock type													
Basalt	0.4		0.7										6.2
Disseminated OX-OL gabbro				38.8	87.2	34.8				25.9		1.6	7.9
Gabbro			1.1					0.1					0.3
Gabbronorite	88.5	19.5	0.6										5.5
Oxide-gabbronorite	6.9	1.3	0.4			5.7							0.7
Oxide gabbro			6.1	1.7	0.6		0.2		0.5			0.1	1.8
Oxide microgabbronorite									6.9				0.3
Olivine gabbro	4.1	79.2	82.3	58.2	2.6	38.2	10.0	99.0	79.7	34.8	39.0	65.3	62.6
Olivine microgabbro			1.6		2.2				1.9	1.6			0.8
Patchy OL gabbro/microgabbro			4.1						6.6	17.9	5.2		2.1
Microgabbro			1.1			0.9							0.3
Oxide-olivine gabbro			1.0	0.5	6.2	18.1	89.0	0.9	4.4	17.0	19.1	24.0	14.9
Oxide-olivine microgabbro							0.8			2.7	14.6		0.4
Troctolite											20.6	9.1	1.9
Troctolitic microgabbro			0.9	0.8	1.1	2.3	0.1				1.6		0.4

Extensive analyses of individual phases are available in Ozawa et al. (this volume).

Textural data were compiled from descriptions of 260 thin sections and macroscopic descriptions of the archived core from 0 to 404 m (bottom of Subunit VIA). Descriptions of Subunits VIB, VIC, and VID are based primarily on thin-section information. The textural descriptions included rock type; degree of deformation; presence of laminations, foliations, and size or modal variations; clinopyroxene and olivine textures; maximum and minimum sizes for plagioclase, olivine, and clinopyroxene; and percentage and texture of oxide minerals. A continuous, 70-m section of olivine gabbro in Unit V was described at a centimeter-scale for average grain sizes, clinopyroxene and olivine textures, and modal or size variations.

Modal data were compiled from shipboard data for point-counted samples. Rock-type identifications are from the revised core descriptions (Dick et al., this volume). Where sufficient analyses existed, only the least-altered (less than 10% secondary minerals) samples were included. The modes reported are all estimated primary mineralogies.

We have tried to quantify the importance of igneous laminations in the section by measuring plagioclase sizes and orientations in a number of thin sections. Plagioclase is a cumulus phase in most of the samples and generally has well-developed albite twinning. Sections were measured with a PC-based video digitizing system in sequential fields of view with a 1:1 macro lens or at 25x magnification in a petrographic microscope, depending upon grain size. Maximum lengths for all plagioclase grains were measured parallel to albite twin contacts (i.e., the measurements are the maximum lengths parallel to (010) in the plane of the thin section). Computer memory was not sufficient to measure individual grain areas; thus, populations have been represented as numbers of grains in a particular length or orientation class.

TEXTURAL AND MINERALOGIC CHARACTERISTICS OF PRINCIPAL ROCK TYPES

The principal igneous rock types in the core, as used here, are olivine gabbro and microgabbro, oxide olivine gabbro, disseminated oxide olivine gabbro, gabbronorite, and troctolite. These lithologies are based on characteristics clearly distinguishable by macroscopic examination of the core, combined with thin section description of representative samples. These lithologies correspond to those used by Dick et al. (this volume).

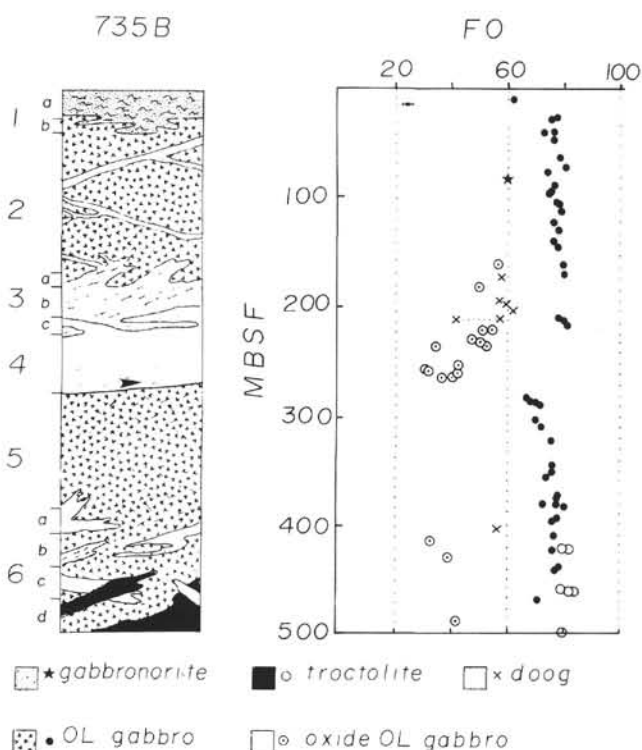


Figure 2. Schematic lithologic section and downcore olivine compositions (OL compositions are averaged core compositions for samples away from intrusive contacts; approximate 2-sigma error bar in upper left). "doog" is a disseminated oxide olivine gabbro (oxide common but less than 2 modal %). Oxide olivine gabbros have greater than 2 modal % oxide. Olivine microgabbros and oxide olivine microgabbros are included with their coarse-grained equivalents. Most of the oxide-bearing units and troctolites appear intrusive into the olivine gabbros. Note the overall homogeneity of the olivine gabbro and the downcore evolution in oxide-bearing gabbros in Units III and IV. The Unit IV/Unit V boundary is adjacent to a thick (about 2 m) mylonitic zone.

Table 3. Average compositions of silicate minerals in principal igneous lithologies (by unit).

Rock type and unit	Plagioclase		Clinopyroxene		Olivine		Orthopyroxene		N
	AVG	STD	AVG	STD	AVG	STD	AVG	STD	
Troctolites									
VIB	66.9	2.3	86.4	1.5	80.8	0.4			3
VIC	69.8	6.3	87.4	0.9	82.0	1.2			6
Troctolitic microgabbro									
IIC	65.1	(2.7)	85.1	(0.8)	82.0	(0.5)			1
Olivine gabbros:									
I	48.1	(3.9)	78.0	(0.5)	61.9	(0.8)			1
IB	60.9	2.0	84.2	0.4	76.4	0.4			3
II	59.7	1.9	81.1	5.9	76.7	2.2	78.6	(2.2)	14
IIIA	60.9	(2.2)	86.0	(0.2)	80.2	(0.2)			1
IIIB	60.1	(0.0)	84.1	(0.7)	78.9	(0.8)	64.6	(1.2)	1
IIC	63.1	(1.6)	84.3	(1.8)	77.6	(0.6)			1
V	59.4	3.0	83.0	2.3	73.4	3.6	77.4	(1.1)	13
VIA	60.4	1.1	82.6	1.4	77.0	0.7			6
VIB	61.2	1.1	84.2	1.7	77.5	1.6			4
VIC	60.0	0.5	83.8	1.6	77.6	0.6			2
OL microgabbro									
II	62.0	5.1	83.0	2.6	76.9	1.6			3
VIA	60.8	0.0	82.4	0.6	75.5	0.1			2
Patchy OL gabbro									
II	59.9	0.5	80.8	3.2	73.0	5.8			2
VIA	60.8	0.7	83.1	0.6	77.0	0.6			3
VIB	66.9	(4.2)	84.5	(0.9)	76.1	(0.5)			1
Gabbronorite									
I	42.2	1.0	70.8	2.0			58.3	0.8	3
II	45.4	(4.5)	71.8	(0.5)	54.8	(0.2)	nd	1	
Microgabbronorite									
VIB	40.6	(1.0)	68.1				60.8	(1.7)	1
Diss. Ox-OL gabbro									
IIIA	43.0	0.9	72.9	1.6	57.1	0.8			3
IIIB	42.9	1.5	72.5	0.4	59.8	2.1			4
IIC	40.5	1.4	70.3	0.4	57.1	2.8			2
VIB	42.4	(1.1)	71.6	(0.4)	56.0	(0.7)			1
OX-OL gabbro									
II	40.6	(0.8)	69.4		55.1				1
IIC	45.4	(4.5)	71.8	(0.5)	54.8	(0.2)			1
IV	34.8	2.6	64.0	3.6	42.0	6.8	54.6	4.0	16
OX-OL microgabbro									
IV	36.7	(0.7)	66.4	(0.1)	46.1	(2.1)			1
VIB	36.5	1.0	63.8	0.7	39.2	0.5			2

Averages are for core compositions. Standard deviations in parentheses are for variation within the single sample. N = the number of samples.

Troctolites contain mostly olivine (OL) and plagioclase (PLAG) with less than 5% clinopyroxene (CPX); troctolitic microgabbros are fine-grained and contain between 5% and 10% CPX. Olivine gabbros contain more than 95% OL, PLAG, and CPX, with trace interstitial amounts of orthopyroxene (OPX), brown amphibole, Fe-Ti oxide, and sulfide. The gabbronorites described here have abundant hypersthene (greater than olivine), appear largely free of primary oxide, and are restricted principally to Subunits IA and IB. Oxide olivine gabbros contain more than 5% Fe-Ti oxide and have modal OL greater than or equal to OPX + pigeonite (PIG). Disseminated oxide olivine gabbros contain less than 2% Fe-Ti oxide and common intergranular OL.

There was unanimity of opinion for naming the more fractionated oxide olivine gabbros, the olivine gabbros, and the troctolites. However, there is some diversity of nomenclature within the disseminated oxide olivine gabbros and less-fractionated oxide-olivine gabbros. Our oxide olivine gabbros include Ozawa et al.'s (this volume) olivine pigeonite gabbros, pigeonite gabbro (gabbronorites with PIG > OPX), interstitial oxide gabbro and olivine oxide gabbro. Our disseminated oxide olivine gabbro designation encompasses Ozawa et al.'s olivine gabbronorites and disseminated oxide-olivine gabbros. This nomenclature problem reflects a real diversity in the least-fractionated oxide-bearing gabbros. In

thin section, many have significant amounts of low-Ca pyroxene. These gabbros, as will be discussed, appear to have crystallized in an interval where magnesian olivine was reacting out to form low-Ca pyroxenes, and iron-rich olivines were crystallizing as an intergranular phase. As a consequence, there is a great deal of fine-scale diversity in modes. Macroscopically, however, there are readily identifiable characteristics about the nine principal lithologies we have chosen to describe the core. Therefore, we discuss the core in terms of those macroscopically defined lithologies, because of their prominence in the core and to keep a correspondence with the detailed lithologic descriptions of Dick et al. (this volume). We discuss the units from the least to the most differentiated (Fig. 3).

Troctolites and Troctolitic Microgabbros

Troctolites occur only in Subunits VIC and VID, where they compose about 10% of the section (Table 2). Troctolitic microgabbros are described in a few places higher in the core; most of those above Unit VI have compositions similar to those of the olivine gabbros. The troctolitic lithologies occur as clearly intrusive veins and dikes cutting both olivine gabbro and oxide-bearing gabbro. The thickest is about 1.5 m wide. There are rare instances in which the troctolites are cut by late-stage oxide gabbros (Dick et al., this volume).

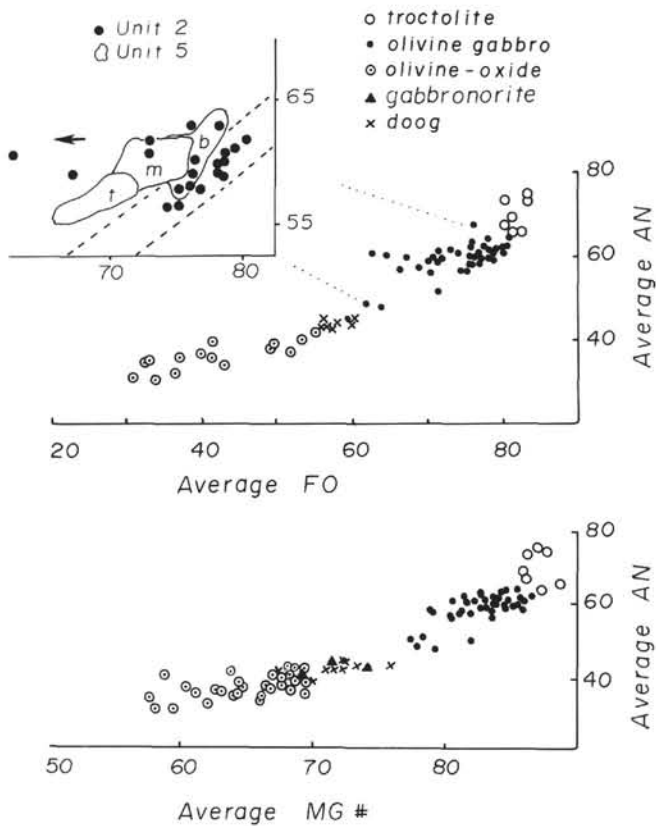


Figure 3. Coexisting OL, PLAG, and CPX average core compositions. Inset shows range of gabbro compositions in Unit V (t = top, m = middle, b = bottom) and Unit VI (solid dots). Dashed lines indicate main trend of gabbroic compositions. Note the overlapping ranges of disseminated oxide olivine gabbro, gabbronorite, and oxide olivine gabbro compositions. Note the diverse trend of Unit II gabbros; the samples that plot to the left (direction of the arrow) are near contacts with oxide olivine gabbros and show evidence of re-equilibration of their mafic phases with more fractionated oxide-bearing liquids.

Troctolites have euhedral (apparently cumulus) to intergranular OL, rare euhedral spinel, and euhedral to intergranular PLAG, with less than 10% intergranular to poikilitic CPX (Pl. 1a). Microgabbros are equigranular. Modal OL in coarse and fine-grained varieties is 20% to 28% (Table 4). None of the troctolites show an igneous lamination, although there is a weak lamination in some of the troctolitic microgabbros. These are the most magnesian rocks in the core. Troctolites have OL of Fo 80 to 83.5, CPX $100 \times \text{Mg}/\text{Mg} + \text{Fe}$ (Mg#) of 85 to 88, and PLAG of An 64 to 75 (Table 3, Fig. 3).

Olivine Gabbros and Microgabbros

The olivine gabbros and olivine microgabbros are treated as a group because of their modal and chemical similarities. They constitute the principal rock type in the core, occurring in every unit and making up over 60% of Units IB, II, V, and VI. The olivine gabbros are medium- to coarse-grained, with euhedral to subhedral OL and PLAG. OL is generally smaller than plagioclase (10 mm compared to 22 mm, Table 5). Olivine gabbros are typically subophitic to ophitic (more than 80% of observations, Table 3, Pls. 1b, 1c). Ophitic to poikilitic CPX (to 7 cm) typically enclose PLAG smaller than those between the CPX.

Olivine microgabbros are fine-grained with equigranular textures. They occur as discrete seams and layers or as irregular pods within olivine gabbro, producing what are termed patchy olivine gabbros (Fig. 4; Robinson, Von Herzen, et al., 1989, p. 127, 130). The patchy olivine gabbro and olivine microgabbro are most abundant in Unit II and Subunits VIA and VIB; they are largely absent in Unit V.

Olivine gabbros have modal OL of 2% to 28% (average 9.8%), PLAG 34% to 68% (average 57%), and CPX 17% to 45% (average 33%). There are no significant modal differences between gabbros and microgabbros (Table 4).

There is no pronounced modal or phase layering in the olivine gabbros. Modal olivine variations occur in some samples (Table 5) as irregular, centimeter-scale concentrations or scarcities. The most common textural variation in the olivine gabbro is defined by grain size changes, but these generally do not define a layering. They can be sharp transitions from olivine gabbros to microgabbros (Fig. 4) or a patchy mixing of coarse and fine gabbros. Measurements in a long section of undeformed olivine gabbro in Unit V show that silicate grain size variations are correlated. Changes in the size range of one phase are mirrored by changes in the others (Fig. 5). This size correlation breaks down only in very coarse intervals with large ophitic CPX. Olivine in those intervals, if present, tends to be small (Fig. 5, 352 m).

The undeformed olivine gabbros typically do not display a prominent igneous lamination (only 25%–30% of observations, Table 5). Orientation data indicate that some of the gabbros have a weak subhorizontal orientation of plagioclase, which is often manifest only in the larger grains (Fig. 6).

Olivine compositions range from Fo 60 to 80, PLAG from An 48 to 66, and CPX Mg# from 77 to 86. OL is homogeneous. PLAG and CPX are both normally and reversely zoned. The CPX zonation is most marked in TiO_2 ; in extreme cases, it may increase from 0.4% to 1% from cores to rim. Plagioclase zoning may be as great as 10 mol% AN. Normal zoning is typical of PLAG in olivine gabbros from Units I, II, and III, while reverse zoning is common in Unit V gabbros. Reverse zoning typifies plagioclase chadacrysts in the undeformed Unit V gabbros.

Mineral compositions are similar in the olivine gabbros and microgabbros and are relatively homogeneous down the core (Table 3; the average olivine gabbro has Fo = 77.3 ± 1.8 , An = 60.6 ± 1.0 , CPX Mg# = 83.7 ± 1.3). Distinctly more fractionated gabbros occur in Units I and III and in the uppermost part of Unit V (Fig. 2, Table 3).

The transitions from olivine gabbro to microgabbro show no sharp modal or compositional changes (Fig. 4). Some samples show a slight evolution in composition across thin sections, but have no sharp discontinuities at the coarse/fine contact (Fig. 4).

Gabbronorites

These rocks occur principally in Unit I as porphyroclastic gabbros interleaved with poorly defined olivine gabbro intervals. Reliable primary modes were difficult to determine because of the degree of deformation and alteration of the cores (Tables 4 and 5). Primary hypersthene appears to have been more than 10% in most; olivine and oxides are minor. The original Unit I is inferred to have been largely coarse-grained because of the common occurrence of coarse (up to 11 mm) CPX porphyroclasts. Plagioclase An contents are 41 to 43, CPX Mg#s are 69 to 75, and OPX Mg#s are 59.

An oxide-rich, olivine-free microgabbro dike occurs in Subunit VIA. It is equigranular with large (8 to 9 mm) OPX oikocrysts and clearly crosscuts the olivine gabbro (Plate 1d).

Table 4. Estimated primary modal mineralogies for igneous lithologies from Hole 735B.

Rock type: N:	Troctolites		OL Gabbro		Gabbronorites		DOOG			OX-OL Gabbro			
	T	TMG	OG	OMG	GN	GNMG	DOOG	PIG	OXOL	OL-RICH	OL	PIG	MG
	2	2	27	4	1	1	6	1	6	1	1	1	1
OL AVG			9.8	12.1	2?		5.1	tr	1.6	20			
OL STD			5.2	6.5			2.8		1.0				
OL MAX	28	19.8	27.0	19			10.0		3				10
OL MIN	25.5	19.8	2.2	6.2			0.9		0.1				5
PL AVG			56.7	53.4	65	57	64.0	59.2	41.6	45	67		
PL STD			7.9	8.9			7.7		5.2		6.5		
PL MAX	68	72.6	68.4	69.9			78.0		51.5		73	50	59
PL MIN	65	64.1	33.5	40.0			57.3		37		58	20.7	45
CPX AVG			33.3	34.4	22	24.7	29.6	2.5	39.8	25	24.3		
CPX STD			6.7	13.0			8.8		6.5		3.4		
CPX MAX	7	16.1	45.0	53.0			36.0		49		29.0	54	40
CPX MIN	4	5.7	17.3	23.7			11.0		31		21.0	30	31
OPX AVG			0.1	tr	10	12	0.6	37.5	1.0		tr		tr
OPX STD			0.1				0.9		0.7				
OPX MAX	1.3		0.5				2.5		2.0			11	
OPX MIN	0		0			tr	0		0.1			9.7	
OPQ AVG		0.5	0.1	tr		5.8	0.9	0.5	16.2	10	8.7		
OPQ STD			0.2				0.6		4.4		3.1		
OPQ MAX	0.1	0.1	1.0				2.2		22.5		13	15.3	6
OPQ MIN	0.1	0.1	0				0.3		10		6	9	5
AMPH AVG	0.9	1.0	0.2		1	0.5ap	1.0	0.2	0.8		nd	0.1	
ALT	7	1.1	4.6	30.5	37	1.3	10.8	9.3	16.5	38	17.9	13.4	nd

These were constructed from samples point-counted during shipboard research. Olivine gabbro averages are constructed from the least altered (<10%) samples. Intervals with only two samples are listed only as a MAX and MIN. Rock codes are OG, olivine gabbro, OMG, olivine microgabbro, T, troctolite, TMG, troctolitic microgabbro, GN, gabbronorite, PIG, oxide-bearing gabbro with pigeonite as the low-Ca pyroxene, DOOG, disseminated olivine-oxide gabbro, OXG, oxide gabbro, OXOL, oxide-olivine gabbro, and GNMG is an oxide microgabbronorite. OL-rich under OX-OPOL gabbros is from a thin olivine-rich interval, MG indicates an oxide olivine microgabbro. tr indicates a trace amount of the phase is present. The OPQ (opaque) row includes principally sulfides for olivine gabbros and troctolites, and ilmenite and magnetite for the other lithologies. The AMPH row includes an estimate of the primary brown hornblende in the samples (or apatite where noted as AP).

Its silicate mineral compositions are An 39, CPX Mg# 65.3, and OPX Mg# 63.4.

Disseminated Oxide Olivine Gabbro

This is a macroscopic descriptive term for a lithologic unit with obvious intergranular olivine and oxides, which comprise less than 2% of the rock. The most common lithology in the unit is an oxide (<2%) and olivine (5% or less) bearing gabbro or gabbronorite. Both hypersthene and pigeonite-bearing varieties have been identified. This lithology occurs as relatively thick intervals in Unit III Subunits VIB and VIC and is the principal constituent of Unit III (Fig. 2, Table 2).

The common textural features are small, intergranular OL (Fo 57 to 63) with dispersed intergranular oxides (ilmenite and Ti-poor magnetite). OL is clearly intergranular to pyroxenes and occurs rimming low-Ca pyroxene (Pl. 1e). CPX (Mg# 70 to 73) and PLAG (An 40 to 43) are granular.

Most samples show moderate deformation, with common grain boundary granulation. Patchy coarse-to-fine grain size changes are common; the coarser sections have 2 to 14 mm PLAG, 2 to 11 mm OL and 3 to 17 mm CPX (Table 5). The rocks typically have a well-developed foliation that dips 20° to 30° and is apparent even in the least-deformed samples (Fig. 7, Pl. 1f). The lamination is clearly defined by the alignment of plagioclase grains of all sizes (Fig. 7).

The disseminated oxide olivine gabbros and their associated lithologies have sudden changes in phase assemblages (appearance or disappearance of pigeonite, hypersthene, and olivine), which do not correspond to changes in mineral compositions (Fig. 8). Some samples show a continuous evolution in mineral composition across the contacts. The diversity of phase assemblages in a narrow compositional range suggests that these samples are crystallizing at or near the magnesian olivine-low-Ca pyroxene peritectic.

Oxide Olivine Gabbros

This lithology is the second most abundant in the core (15%). It occurs as veins and seams in Units II, III, and VI and constitutes the bulk of Unit IV (Table 2). It forms sharp contacts with the olivine gabbro, sometimes truncating plagioclase crystals in the olivine gabbro (Ozawa et al., this volume) or enclosing clasts of olivine gabbro in olivine oxide gabbro (Pl. 1g; Dick et al., this volume). The lithology is defined by abundant oxides (>5%), common olivine, and a pronounced foliation (Pl. 1h). Modal olivine abundance varies from less than 1% to 20%. Oxides make up 1% to 20% (locally to 50%) of the sample. Some samples are pyroxene-rich, with up to 50% CPX. OPX is common at about 1 modal %; in some samples, it is sufficiently abundant to term the sample an olivine gabbronorite (Fig. 9). Oxide abundances are constant or show a slight decrease downward within Unit IV (Fig. 9). The lowermost sections of Unit IV tend to be more olivine rich than the upper parts.

The typical lithology is granular with pronounced coarse-to-fine size variations (Fig. 8). In places, oxide olivine microgabbros form pods or veins; these are modally and compositionally similar to the coarse-grained facies. Most of the samples exhibit a moderate deformation, with undulose pyroxene and grain boundary granulation and recrystallization. PLAG sizes range from 1 to 16 mm, CPX from 2 to 43 mm, and olivine from 1 to 10 mm (Table 5). Olivines are intergranular or poikilitic to granular. No consistent changes occur in grain size with depth.

Plagioclase compositions range from An 35 to 38, CPX Mg# from 58 to 70, and OL from Fo 30 to Fo 55. Oxides are principally ilmenite and Ti-poor magnetite. Olivines are normally unzoned, while CPX shows slight to moderate reverse and normal zoning (1 to 5 Mg#). Plagioclase in Unit III and at

Table 5. Petrographic and textural characteristics of the five principal igneous lithologies from Hole 735B.

Rock type	Troctolite	OL Gabbro	Gabbronorite	DOOG	OLOX
N of observations	13	396	19	28	58
Deformation P	—	2	100	nd	—
H	—	6.7	—	nd	85
CPX texture O/SO	nd	72	—	—	—
P	nd	2.4	68	—	—
G	nd	26	24	95	80
Size variations	23	15	0	43	27
Modal variations (OL)	23	21	5	11	16
Orientation	—	29	100*	37	50
CPX AVG MAX	nd	22.6	10.9	16.7	16.1
STD MAX	nd	7.4	3.1	6.4	8.1
AVG MIN	nd	1.6	nd	2.8	3.2
OL AVG MAX	nd	10.0	—	10.7	7.8
STD MAX	nd	1.7	—	6.0	2.8
AVG MIN	nd	1.6	—	1.9	2.0
PLAG AVG MAX	6.9	22.3	4.3	14.2	14.3
STD MAX	1.1	2.6	3.2	6.7	6.6
AVG MIN	1.1	1.6	<1	2.2	2.4

(—) indicates the characteristic was not noted, nd indicates that it was not determined for that rock type in that interval. N = the number of observations within each interval; textural features, except for grain sizes, are expressed as a percentage of occurrence for the number of observations. Other notations are P, porphyroclastic textures; H, highly deformed; O/SO ophitic/subophitic; G = granular, P = porphyroclastic, size variations refer to irregular coarse-fine mixtures. Orientation refers to an observation of a distinct planar fabric in one or more minerals, which indicates orientation results from deformation. Grain size data include AVG MAX, the average of the maximum grain sizes; STD, the standard deviation of the maximum grain sizes; and AVG MIN, the average minimum grain size in the interval. Alteration (%) is from the thin section modes. DOOG = disseminated oxide olivine gabbro, OLOX = oxide olivine gabbro.

the top of Unit IV are reversely zoned, with rims up to 6 mol% more calcic than cores. The lowermost samples in Unit IV typically are normally zoned up to 5 mol% An. A pronounced fractionation of the olivine oxide gabbros occurs downward in Unit IV (Fig. 2).

The oxide olivine gabbros exhibit a prominent foliation, even in least deformed samples (Pl. 1h, Fig. 10), much like that observed in the disseminated oxide olivine gabbros. Dick et al. (this volume) documented a flattening downward of this foliation within Units III and IV.

Other Lithologies

A metabasalt dike cuts the core in Unit II; a deformed metabasalt was identified in Unit I on geochemical grounds (Robinson, Von Herzen, et al., 1989). Robinson, Von Herzen, et al. (1989) identified both.

A trondhjemitic intrusion breccia occurs near the base of Unit IV; minor trondhjemitic veins are present in several places in the core. The distribution and characteristics of the trondhjemites are described elsewhere (Dick et al., this volume).

DISCUSSION

Several features of the gabbros from Site 735B should be noted. First, the mineral compositions of the gabbros span a wide range, from very magnesian troctolites to very fractionated Fe-Ti oxide gabbros. Their compositions define a curved trend subparallel to a tholeiitic liquid line of descent (Fig. 3). Despite this generally coherent trend, however, the distribution of rock compositions in the core overall is roughly bimodal: it constitutes principally olivine gabbro with OL of Fo 77 ± 2 and intervals of oxide-bearing gabbro with OL of Fo less than 60 (Fig. 2). This bimodality is particularly evident when the percentage of core within compositional bins is plotted (Fig. 11). Two systematic changes are superimposed on this bimodal distribution. The first is the downcore fractionation of oxide-bearing gabbros in Units III and IV, and the

second is the shift of olivine gabbros to more Fe-rich compositions at the top of Unit V (Fig. 2).

Relationships Between Rock Types

The clearest relationship between rock types is that between the olivine gabbros and the oxide-bearing gabbros (inclusive of disseminated oxide olivine gabbros and oxide olivine gabbros). In nearly all cases, the latter appear intrusive into the former. Olivine gabbros near these contacts commonly have disequilibrium mineral compositions (more Fe-rich olivine or CPX at a given plagioclase composition, Fig. 3, Ozawa et al., this volume). Oxide-bearing gabbros can be found truncating olivine gabbros and enclosing clasts and fragments of olivine gabbro. The oxide gabbros typically have a prominent foliation that occurs variously in deformed and less-deformed samples. Nonfoliated olivine gabbro clasts also are found in foliated oxide-bearing gabbro. These two observations indicate that the foliation is in large part a magmatic flow foliation, imparted as the rocks were intruded as a crystal-liquid mixture. Dick et al. (this volume) have postulated that the intrusion of the oxide gabbros and the beginning of brittle-ductile deformation of the section are closely linked, and that the deformation both provided porosity for the ferrous liquids and helped to separate them from the olivine gabbro pile.

This relationship of intrusion of oxide-rich crystal mushes or liquids holds true for the entire range of oxide-bearing compositions (oxide olivine gabbros and disseminated oxide olivine gabbros). These liquids were fractionating as they were emplaced and cooled.

The troctolites are also clearly intrusive into the lowest parts of the olivine gabbro (Fig. 2; Dick et al., this volume). These have sharp but irregular contacts with the olivine gabbro, form well-defined, cross-cutting layers, and in places have produced Cr-rich diopsides in the olivine gabbros by reaction (Dick et al., this volume). The relationship of the troctolites to the oxide gabbros is less clear. In most cases, the

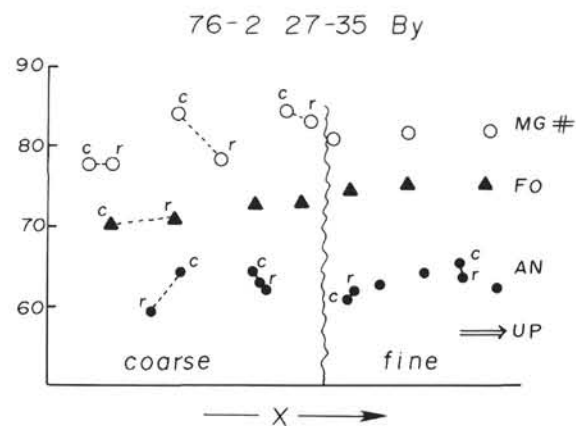
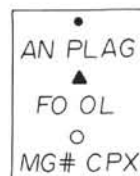
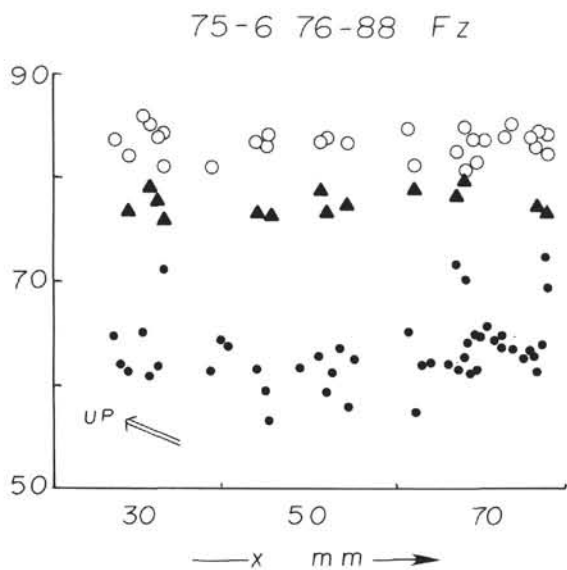
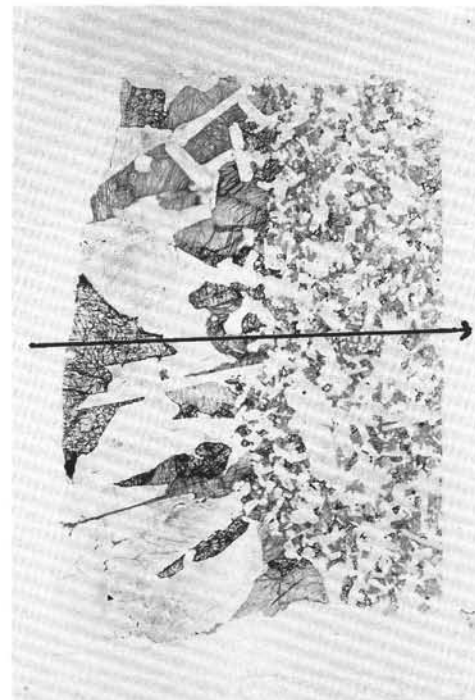
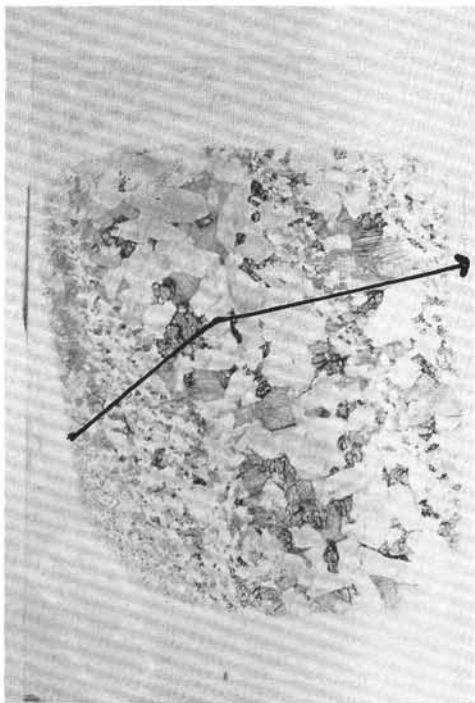


Figure 4. Contacts in a patchy olivine gabbro (left, Subunit IVA) and a coarse-grained olivine gabbro and olivine microgabbro (right, Subunit VIA). Both sections are 5 cm wide. In this and subsequent figures the analyses (points or traverses along the dotted lines) are projected onto a line whose orientation is shown by the solid line and arrow in the photographs. The approximate location of the textural boundary in that projection is shown in the plot by an irregular line.

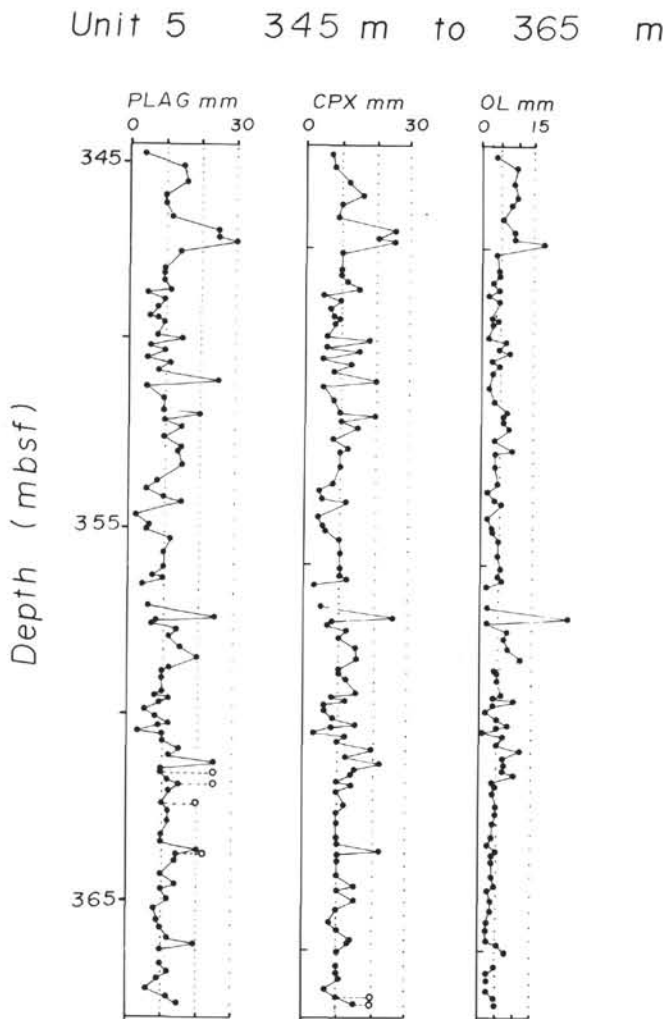


Figure 5. Size variations in part of a 70-m section of olivine gabbro in Unit V. Sizes are estimated averages for each phase. Open circles indicate anomalously large grains in an otherwise homogenous interval.

troctolites cut olivine gabbros that appear to have been intruded already by an oxide gabbro. There is some evidence, however, that some of the troctolites are cut by late-stage oxide-bearing gabbros (Dick et al., this volume). It appears that in the lower part of the core the episodes of troctolite and oxide-bearing gabbro intrusion overlapped.

Variations Within Rock Types

No well-developed modal or phase layering is found in any of the gabbros in the Hole 735B cores. In fact, the olivine gabbro is somewhat remarkable in its compositional homogeneity. Some sharp changes are found in the assemblage or modes, but these are localized. The rhythmic layering described in so many ophiolites and layered complexes (e.g., Campbell, 1978; McBirney and Noyes, 1979; Wager and Brown, 1967) is absent here. The most common petrographic variation in the core (it is found within olivine gabbros, oxide-bearing gabbros, and troctolites) is an irregular coarse-to fine grain size transition (Pl. 1, Figs. 4, 8). This variation occurs as discrete layers of microgabbro within gabbro or mixed pods and patches of microgabbro within gabbro. Most of these changes are not marked by any compositional change. On a scale of centimeters to a meter, subtle

variations are found at most in mineral compositions. Little evidence exists for the type of regular mineral resets described in gabbros from the Oman ophiolite and similar bodies (e.g., Browning, 1984). The size variations are similar to the patchy coarse-fine segregations described in some high-level ophiolitic gabbros (Ernewein et al., 1988), though the compositions of the two are very different. The high-level ophiolitic gabbros most commonly are compositionally uniform amphibole gabbros.

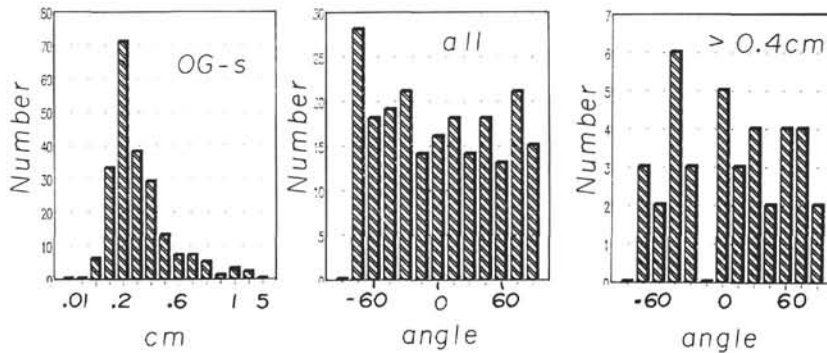
Little evidence can be seen of hydrodynamic crystal sorting in the olivine gabbros. A long olivine gabbro section in Unit V shows co-variation of olivine, plagioclase, and clinopyroxene grain sizes throughout, with the olivine typically one-half the size of the plagioclase and clinopyroxene (Fig. 5). The absence of any density sorting and regular co-variation of sizes suggest *in-situ* nucleation and growth of the cumulus phases along the margins of a chamber (e.g., Campbell, 1978; McBirney and Noyes, 1979).

An interpretation of *in-situ* crystallization for the olivine gabbro is supported by the modal data. The best-constrained modes for the olivine gabbros are 8% to 9% OL, 57% to 58% PLAG, and 32% to 34% CPX. These are near modes estimated from 1-atm experiments or least-squares modeling of tholeiitic basalt differentiation. The 1-atm experiments on primitive basaltic compositions give modes of 11% OL, 61% PLAG, and 28% CPX (derived from sample runs 12 and 17 on P12 of Walker et al., 1979). Least-squares modeling of fractionation for the more primitive Galapagos Rift basalts (Clague and Bunch, 1976) produces modes for cumulate gabbros that range from 3% to 9% OL, 52% to 63% PL, and 30% to 45% CPX.

If the olivine gabbro formed by *in-situ* crystallization, the sudden grain size changes may reflect intrusions of crystal mushes or changes in conditions of crystallization. In the former case some compositional difference in cumulus phases might be expected across the contact. These are not obvious in the Hole 735B samples (Fig. 4). Post-cumulus re-equilibration will modify mineral compositions, and evidence of initially different cumulus compositions may have been erased by intermingling of intercumulus liquids and subsequent re-equilibration. We do not think that this is the case for several reasons. On a scale of a meter or so through the zones, where we have taken sequential samples, mineral compositions remain constant regardless of proximity to the contact. There is no evidence of a mixing or offset zone. No indications of pronounced zoning in feldspars near the contacts is found, and the amounts of intercumulus liquid are nearly identical in both fine- and coarse-grained lithologies (Meyer et al., unpubl. data). This would not be the case if the finer-grained half were a "chilled" intrusive body with elevated growth rates. Silicate phases have homogeneous minor element (Cr, Ti, Ni), as well as major element, compositions in the coarse- and fine-grained intervals. All these observations suggest that the uniformity of composition of the coarse and fine intervals is not the result of a post-cumulus homogenization of initially different cumulus cores, but rather reflects crystallization from liquids of similar composition.

We interpret most of these within lithology textural changes as the products of various growth and nucleation rates. It is difficult to constrain either of these parameters. The similar trapped liquid amounts in the coarse and fine portions of some samples suggests that the growth rates were not much different, as rapid growth would tend to produce higher trapped liquid concentrations. The relative sizes of the olivine, plagioclase, and pyroxene suggest somewhat slower growth rates for the olivine, as they are consistently smaller than the co-existing silicates. Measured peak growth rates for the three silicates are similar (10^{-5} cm/s for plagioclase, $2.5 \times$

76-2 16-26



62-4 89-99

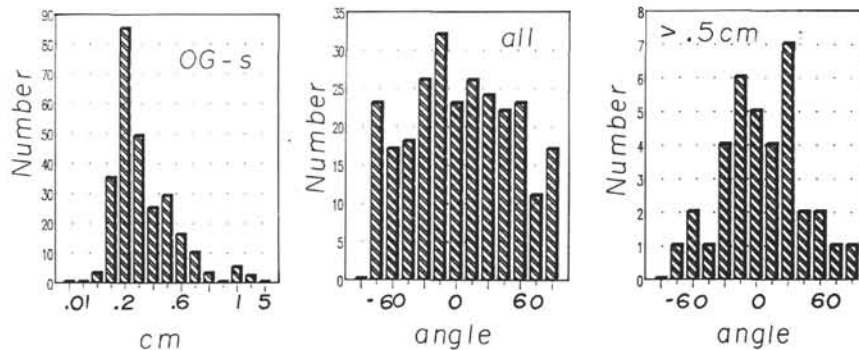


Figure 6. Size and orientation histograms for plagioclase populations in selected samples of olivine gabbros. The plot farthest right is an orientation histogram that includes only grains larger than the specified size. OG is olivine gabbro, s indicates slightly deformed (some undulose extinction, minor grain bending or fracture). The top figure, with no prominent lamination, is most typical of the olivine gabbros as a whole.

10^{-5} for olivine, and 9×10^{-5} for diopside) (Dowty, 1980); however, peak growth rates for pure systems may have little applicability to multicomponent, natural systems. Measurements of growth rates of minerals from lava lakes indicate very slow growth ($2-11 \times 10^{-10}$ cm/s) and suggest small degrees of undercooling (Kirkpatrick, 1977). The textures and grain sizes of the Hole 735B samples suggest heterogeneous nucleation of the silicate phases and significantly slower growth for the olivines. Data for numbers of grains per cubic centimeter, as well as precise modes, on coarse- and fine-grained intervals are required if we are to quantify any of these rates.

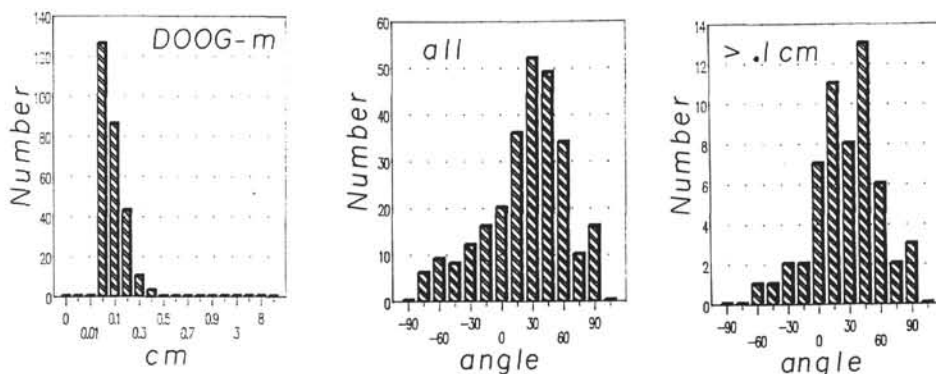
If we assume, by analogy to lava lakes, that undercoolings in oceanic magma chambers are low and growth rates are low, it seems that an explanation of the changes in grain size may lie in changes in nucleation rates. Peak nucleation rates are generally at different undercoolings than peak growth rates (Dowty, 1980). Unfortunately, experimental work on nucleation rates faces most of the same problems as experimental estimates of growth rates. Study of lava lakes clearly shows that most nucleation is heterogeneous and, despite generally small undercoolings, covers a tremendous range (7×10^{-3} nuclei/cm³/s to 2 nuclei/cm³/s; Kirkpatrick, 1977). A three order-of-magnitude change in nuclei density might easily

produce pronounced changes in grain size along a crystallizing front.

Crystal density might be redistributed along intrusion margins by local slumping or by development of crystal-rich plumes (Marsh, 1988). Indeed, some of the sharp coarse/fine contacts, or the "patchy" (mixed microgabbro and gabbro) olivine gabbros may be the products of such redistribution. The finer-grained intervals would be intrusive in a local sense, but both coarse and fine intervals would be derived from liquids of similar compositions.

The average composition of the olivine gabbros is constant throughout the core (Fo 77, An 61, CPX Mg# 84). The homogeneous compositions suggest that the bulk of the gabbros formed by equilibrium crystallization. The only consistent vertical change in these gabbros is the slight increase in fractionation at the top of Unit V (Fig. 2). The top of Unit V abuts the most fractionated oxide-bearing gabbros. The mafic phases in Unit V are more Fe-rich than their corresponding plagioclase compositions would indicate (compositions are offset to the left in Fig. 3). One possible explanation is that large-scale re-equilibration of the upper part of Unit V has occurred because of the intrusion of the fractionated oxide-olivine gabbros. Note that a major fault is found near the Unit IV/Unit V boundary, and significant

43-1 22-29



77-2 4-7

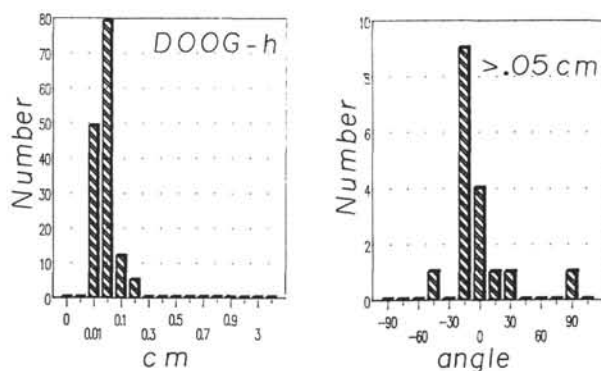


Figure 7. Size and orientation histograms for plagioclase populations in selected samples of disseminated oxide olivine gabbros. The plots farthest right were sorted for larger grains. "m" indicates moderate deformation (kinked twins, undulose extinction, grain boundary granulation), "h" represents high deformation (significant recrystallization of neoblasts). The foliation is well defined, even at lower degrees of deformation (top).

displacement and shortening of the section may have taken place along that fault.

The oxide-bearing gabbros, judging from their foliations, were intruded as crystal-rich mushes. Because grains in the olivine gabbro were truncated by the intrusions and the limited distances to which fractionated liquids penetrated into most olivine gabbros (Ozawa et al., this volume), the olivine gabbros were nearly completely solidified or were at least relatively impermeable, when the oxide-bearing gabbros were intruded. The exception seems to be at the top of Unit V, perhaps because of the magnitude of the compositional difference between the two rock types. These intrusive bodies range from small veins to the 100-m-thick interval that makes up Units III and IV.

It is hard to assess how closely the modes of the oxide-bearing gabbros match cotectic proportions because little experimental or modal data exist about equivalent fractionated melts. The disseminated oxide olivine gabbros (7% OL, 64% PLAG, 26% CPX, 1% OPX, 1% OPQ) are, in many cases, similar to cumulate modes calculated from solutions to low-pressure fractionation of fractionated basalts (Clague and Bunch, 1976) and are probably, as in the case of olivine gabbros, the products of *in-situ* crystallization. The oxide

olivine gabbros, however, have variable modes. Overall, Unit IV has 10.5% oxides, but these range from 3% to more than 55% (Fig. 10, Table 4, Ozawa et al., this volume). OL modes are <1% to 55%, but average under 10% for most of Unit IV, and orthopyroxene averages less than 5%. The only experiments on fractionated tholeiitic liquids (Juster et al., 1989) produced assemblages with 0% to 5% magnetite, up to 25% low-Ca pyroxene, and no fayalitic olivine. These liquids also have much lower Na/Ca ratios than the liquids from which the Hole 735B gabbros crystallized. The drastic difference in phase proportions between the experiments and the Hole 735B gabbros suggests a compositional or P-T-fO₂ control on the appearance of fayalitic olivine vs. low-Ca pyroxene, which was not identified.

At the least, the local concentrations of oxide (more than 10%) must reflect noncotectic proportions as *normative* ilmenite and magnetite in ferrogabbros and ferroandesites from the Galapagos Rift does not exceed 7% or 8% (Fornari et al., 1981; Perfit and Fornari, 1981). The elevated oxide percentages in the oxide olivine gabbros require some local concentration by density or flow sorting, subsolidus redistribution (possibly as a consequence of the deformation of the section), or by development of late-stage immiscible Fe-rich liquids (as

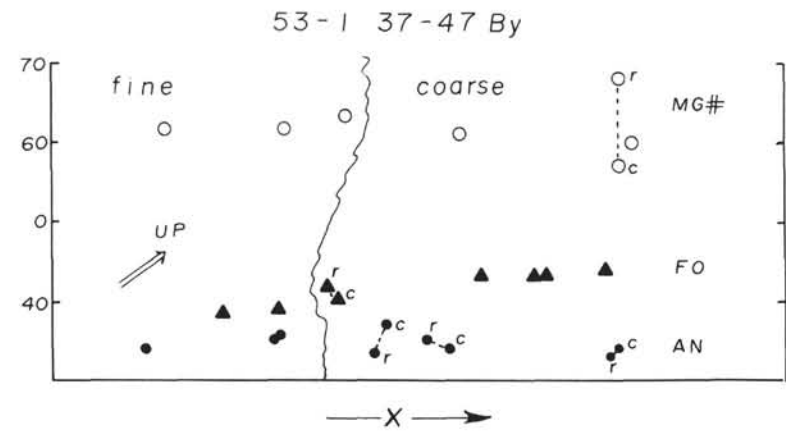
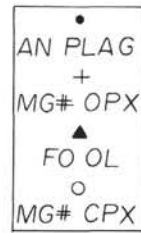
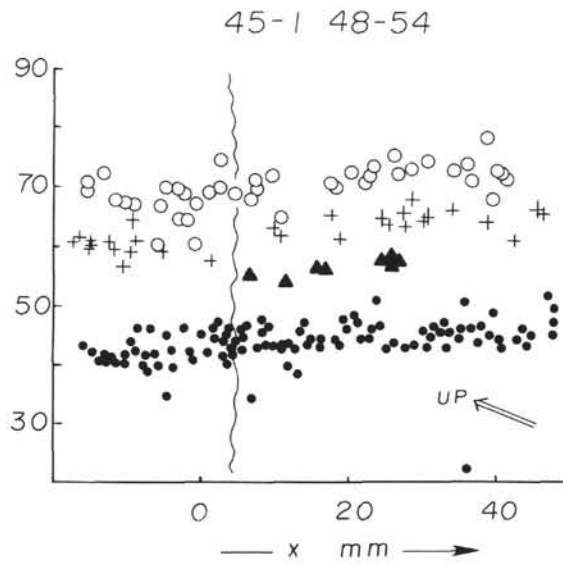
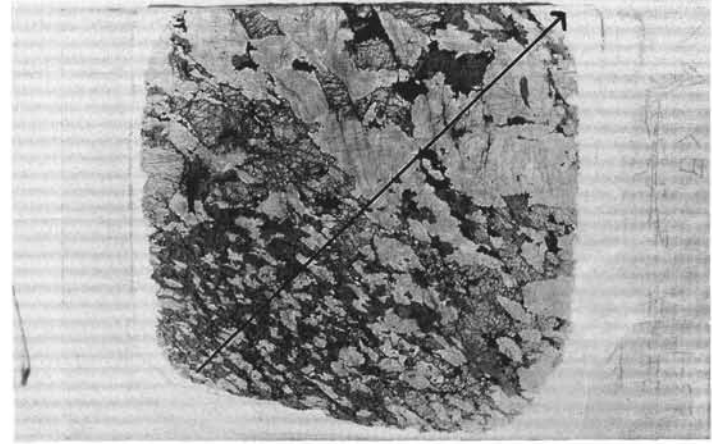
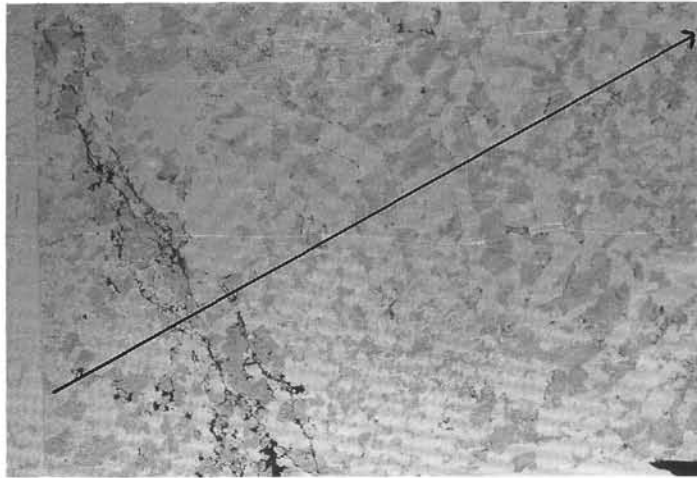


Figure 8. Contacts between fine- and coarse-grained olivine oxide gabbros (right, Unit IV) and pigeonite-oxide gabbro and disseminated oxide olivine gabbro (left, Subunit IIIC). Note the oxide seam along the contact. Both sections are 5 cm wide.

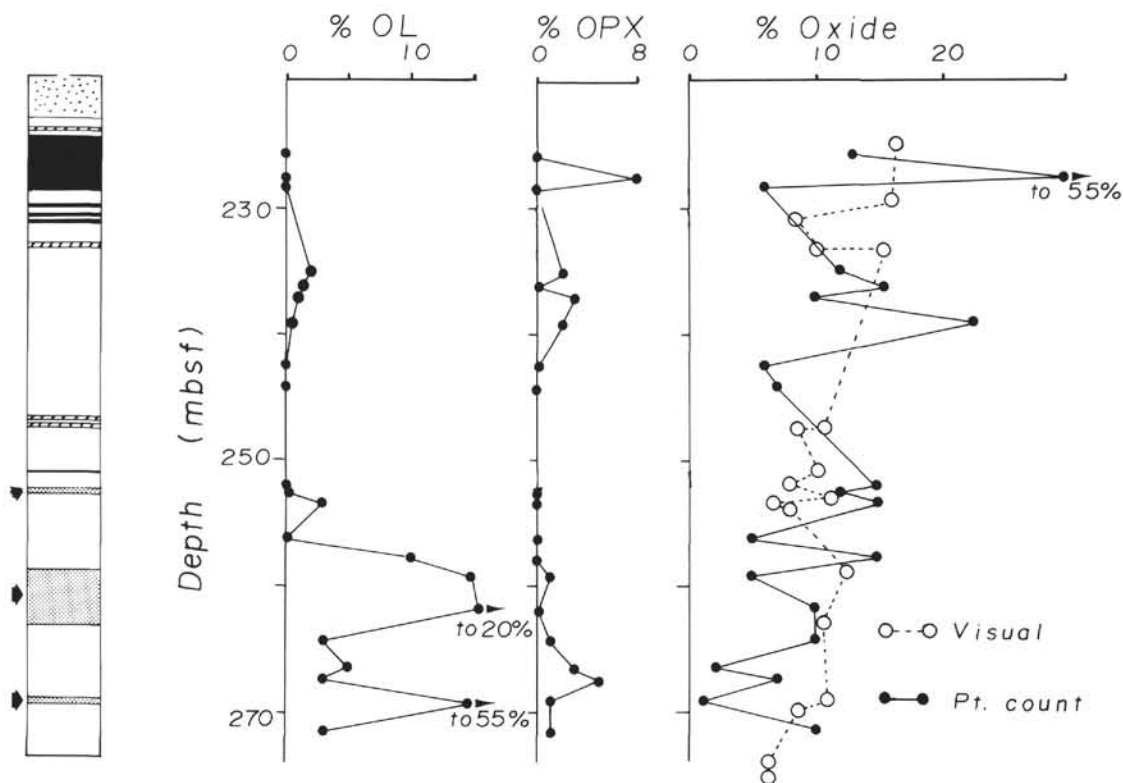


Figure 9. Modal variations of olivine oxide gabbro in Unit IV, including both point counted and visual modes (from core redescription) for reference. The left column is based on the core redescription. Black = olivine gabbros, white = olivine oxide gabbros, stippled = olivine-rich oxide gabbros, lined = olivine oxide microgabbros, and coarsely dotted = mixed olivine gabbro, olivine oxide gabbro, and disseminated olivine oxide gabbro. Note the diversity in modal proportions of OL and OPX; this is reflected in the diversity of nomenclature for rocks in this unit.

postulated by Natland et al., this volume). However, this redistribution need only be local. The average mode for oxide-bearing gabbros in Units III and IV is 5% OL, 37% CPX, 50% PLAG, 6% oxide, and 1.5% OPX. These are not unreasonable values for cotectic proportions (Clague and Bunch, 1976; Juster et al., 1989).

The downward evolution of the rocks in those units is consistent with crystallization of an initially homogeneous crystal-melt mixture, downward from the roof of the intrusion, as has been described in the marginal zones of layered intrusions (Campbell, 1978; Wager and Brown, 1967). The asymmetry of the compositions of the oxide-bearing gabbros may reflect more rapid growth downward rather than upward, combined with some removal of the section along the mylonitic zone at the base of Unit IV. The emplacement of the oxide-bearing gabbros that make up Units III and IV may have been as a single body, or as a series of dikes and sills of progressively more fractionated compositions that filled porosity created as the section was deformed. Structural and textural data suggest that the latter case is the more likely (Dick et al., this volume).

Genetic Relationships Between the Rock Types

The two major lithologies in the core—olivine gabbros and oxide-bearing gabbros—are locally juxtaposed on intrusive contacts. At first glance, the pronounced bimodality of the core (Fig. 11) suggests that this reflects intrusion of a second liquid from an adjacent intrusion into an already cooled olivine gabbro section. Two points should be raised about this scenario.

First, the mineral compositions of the gabbroic rocks, despite the numerical bimodality of compositions, do span a relatively continuous range of compositions (Fig. 3). Calculations of percentages of trapped liquids in these gabbros (Meyer et al., unpubl. data) range from 5% to 15%. This indicates that all of the gabbros—oxide-free and oxide-bearing—are adcumulates and mesocumulates. The offset of cumulate core compositions (only core compositions have been used here) was estimated as at most 1.5 to 3 mol% because of post-cumulus re-equilibration (Meyer et al., 1989). Thus, we can assume that these mineral compositions reflect near equilibrium trends, complementary to a tholeiitic liquid line of descent.

The phase assemblages in the gabbros in the core reflect their changes in composition. The troctolites have cumulate OL + PLAG, and the olivine gabbros have cumulate OL + CPX + PLAG. The disseminated oxide olivine gabbros mark the beginning of reaction of magnesian olivine to form low-Ca pyroxene, with subsequent crystallization of iron-olivine. The onset of this reaction is about at Fo 61 and An 50 (the oxide-free gabbroites). Hypersthene is the first low-Ca pyroxene to appear, followed shortly by pigeonite, followed by Fe-rich olivine. The reaction is reflected in the complex lithologies of the disseminated oxide olivine gabbros and the more magnesian olivine oxide gabbros. The reaction persists to about Fo 50 and An 40, where PLAG + CPX + oxide + Fe-rich olivine (commonly with apatite) become the characteristic crystallizing assemblage. The compositional trends, and phase assemblages, of the gabbros from Hole 735B are similar to those observed in the Skaergaard Intrusion (Wager and Brown, 1967; Naslund, 1976).

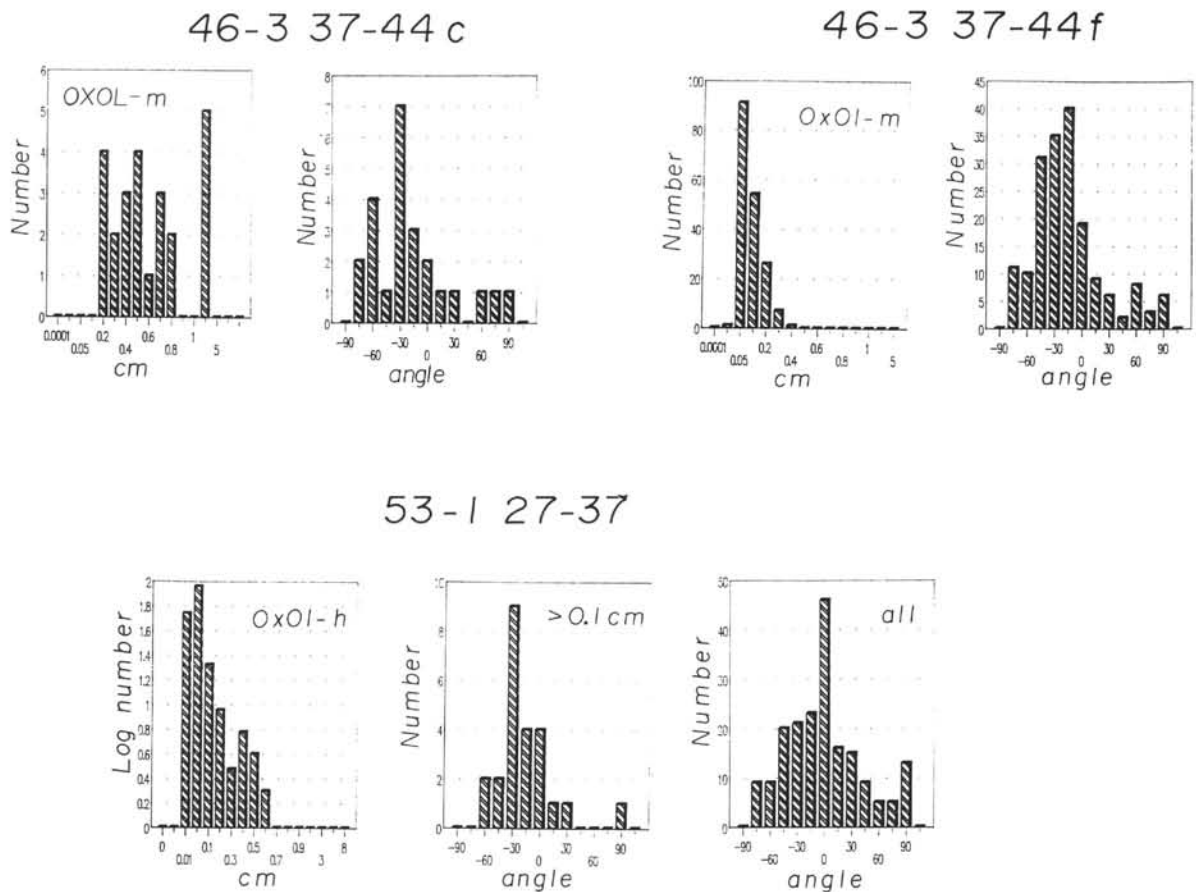


Figure 10. Size and orientation histograms for plagioclase populations in selected samples of oxide olivine gabbros. Some of the size histograms are sorted to include only larger grain sizes. "m" indicates moderate deformation (kinked twins, undulose extinction, grain boundary granulation), "h" high deformation (significant recrystallization of neoblasts). The foliation is well defined even at lower degrees of deformation (top).

This inferred equilibrium line of descent suggests a genetic link between the olivine gabbros and the oxide-bearing gabbros. However, that genetic link might be crystallization from a single body of melt, or intrusion of melts and cumulates derived from two compositionally similar intrusions. The latter case would be expected to produce a variety of intrusive relationships—olivine gabbros cutting earlier olivine gabbros, oxide-bearing gabbros cutting olivine gabbro, and so forth. The clearest evidence for multiple batches of melt should be earlier (more magnesian) cumulates cutting later (more ferrous) cumulates. Indeed, the troctolites cutting the olivine gabbros and oxide-bearing gabbros in Unit VI must have derived from a second intrusive body because their solidus temperatures are higher than the liquidus temperatures of some of the rocks they cut. Other than the troctolites, however, no evidence of such earlier/late intrusive relationships can be seen.

The olivine and oxide-bearing gabbros from Hole 735B also show a definite link between lithologic composition and lithologic structure. The oxide-bearing units are intrusive and are preferentially deformed. No case of a clearly intrusive olivine gabbro or microgabbro can be seen anywhere in the core. The crystallization of the oxide-gabbros was clearly syndeformation to post-deformation, and Dick et al., (this volume) used this as evidence that the intrusion and separation of the oxide-bearing gabbros from the olivine gabbros was driven by deformation of the cumulate pile.

The simplest interpretation of the evidence is that the oxide-bearing gabbros and olivine gabbros derived from a single intrusive body and that the oxide-bearing gabbros have been locally mobilized and intruded as the near-rigid cumulate section began to deform.

If then, these gabbros crystallized from a single body of melt, why are they so strongly bimodal? A certain degree of bimodality is a likely consequence of fractionation of small magma bodies. As long as the olivine gabbro cumulates are interconnected with the residual melt they will follow an equilibrium crystallization path, producing a nearly unimodal range of mineral compositions. The residual liquid will change slowly, as it is buffered by a large mass of crystals. If the gabbro pile becomes impermeable at some point, or if the residual liquid is forced out of the pile by deformation, this buffering effect ceases. While the residual melts are initially in equilibrium with the olivine gabbro, once they are removed from the cumulates, their compositions will evolve rapidly as their temperature drops (particularly if there is a change in the crystallizing phase assemblage), and the cumulate compositions will be displaced rapidly from those of the olivine gabbros. The effect will be to produce a unimodal olivine gabbro section, a gap with few cumulate compositions, and a broad peak of fractionated cumulate compositions. This gap marks the transition from equilibrium to fractional crystallization. Indeed, this is much the pattern that we see in the Hole 735B gabbros (Fig. 11).

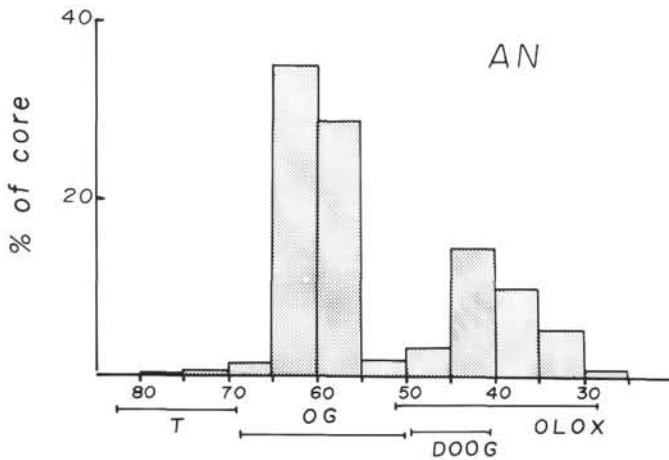


Figure 11. Percentages of rock types in 5 mol% An plagioclase bins. Constructed from average mineral compositions and lithologic thicknesses in each unit. T = the range of compositions in troctolites, OG in olivine gabbros, DOOG in disseminated oxide olivine gabbros, OLOX in olivine oxide gabbros.

Thus, the bimodality is not necessarily a consequence of the mixing by intrusion of two unrelated magma or mushes. With the available evidence, we cannot rule out such a case. However, as discussed, no textural or compositional evidence exists that requires such an interpretation. The oxide gabbros clearly are intrusive into the olivine gabbros. That intrusion is probably a local phenomenon and is a consequence of the residual liquid from crystallization of the olivine gabbro being mobilized into the section as the crust was deformed (Dick et al., this volume).

Model for the Development of the Hole 735B Section

One possible model for the crystallization of the section at Hole 735B is shown in Figure 12. A melt with Mg/Mg+Fe²⁺ of about 0.65, which probably crystallized some troctolites on its way to higher crustal levels, intruded and filled an irregularly shaped chamber by a gabbronorite from an earlier, though compositionally similar, magma body. This melt crystallized along the irregular margins of the chamber. Local thermal perturbations produced locally coarser- and finer-grained pods and layers, which slumped or flowed into adjacent segments. This effect was particularly pronounced in the more marginal facies, where thermal gradients were most extreme. These areas correspond to the olivine gabbros, patchy olivine gabbros, and microgabbros in Units II and VI. The massive olivine gabbro of Unit V represents a more interior facies. The olivine gabbro maintained a thorough intercommunication with the residual melt, as reflected by its homogeneous composition. At about 60% crystallization, the olivine gabbro had formed a rigid crystal-supported network, and subsequent crystallization started to close porosity. As the olivine gabbro section began to deform and to become impermeable, the pods of trapped residual liquid began to evolve rapidly. As the now near-rigid section moved away from the ridge crest, it was cut by listric near-ridge faults that focused the distribution of the late liquids in deformation zones (see Dick et al., this volume). This deformation enhanced pooling of many smaller pockets of these liquids to produce the large intrusion that now make up Units IV and III. The thermal difference between the roof and floor of this intrusion promoted more rapid crystallization at the top than at the floor and produced the downward fractionation observed in Units III and IV (see Ozawa et al., this volume). Some intercumulus exchange may have taken

place between these fractionated liquids and the olivine gabbros at the top of Unit V. At the latest stages of fractionation at the base of Unit IV, a trondhjemitic vein network was emplaced near the Unit IV/Unit V contact.

In the waning stages of deformation, a second intrusion emplaced troctolites into the lower part of the section. Complex histories of hydrothermal alteration and deformation are occurring during nearly all phases of this igneous crystallization.

The section at Hole 735B can be interpreted as the product of near-closed system crystallization of a small magma body. A similar conclusion was reached for gabbroic rocks from fracture zones in the Central Indian Ridge (Bloomer et al., 1989). The textures in these gabbros suggest that within units, *in-situ* crystallization was the dominant process. Compositions more fractionated than olivine gabbro were emplaced by sequential intrusion into earlier cumulates, synchronous with deformation of the near-rigid olivine gabbro. The short-scale diversity in composition and texture of these gabbroic rocks shows them to be more similar to many Appennine ophiolites (Serri, 1980) than to the large, more homogeneous, gabbroic bodies described from ophiolites like those in Oman (Juteau et al., 1988).

ACKNOWLEDGMENTS

We thank the staff and crew of the *JOIDES Resolution* and the Ocean Drilling Program for their skilled and enthusiastic work during the Leg 118 drilling. They completed an outstanding hole in a short period of time. The assistance of Steve Recca at Massachusetts Institute of Technology and Beth Holmburg at the Smithsonian Observatory was invaluable for completing the probe analyses. Frank von Esse and Linda Angeloni provided careful and patient help in the laboratory. Patricia deGroot, Paige Embry, and Bill Bobrowski collected most of the image analysis data. Particular thanks are extended to the staff of the Gulf Coast Core Repository at College Station for their help and patience while we re-described the core.

REFERENCES

- Batiza, R., and Vanko, D. A. 1985. Petrologic evolution of large failed rifts in the eastern Pacific: petrology of volcanic and plutonic rocks from the Mathematician Ridge area and the Guadalupe Trough. *J. Petrol.*, 26:564-602.
- Bloomer, S. H., Natland, J. H., and Fisher, R. L. 1989. Mineral relationships in gabbroic rocks from fracture zones of Indian Ocean Ridges: evidence for extensive fractionation, parental diversity, and boundary layer recrystallization. In Saunders, A. D., and dNorry, M. J. (Eds.), *Magmatism in the Ocean Basin*. Geol. Soc. London Spec. Publ., 42:107-124.
- Browning, P. 1984. Cryptic variation within the Cumulate Sequence of the Oman ophiolite: magma chamber depth and petrological implications. In Gass, I. G., Lippard, S. J., and Shelton (Eds.), *Ophiolites and Ocean Lithosphere*. Geol. Soc. London Spec. Publ., 14:71-82.
- Campbell, I. H. 1978. Some problems with the cumulus theory. *Lithos*, 11:311-323.
- Clague, D. A., and Bunch, T. E., 1976. Formation of feroobasalt at East Pacific midocean spreading centers. *J. Geophys. Res.*, 81:4247-4256.
- Dowty, E. 1980. Crystal growth and nucleation theory and the numerical simulation of igneous crystallization. In Hargraves, R. B. (Ed.), *Physics of Magmatic Processes*. Princeton, NJ (Princeton Univ. Press), 419-486.
- Elthon, D. 1987. Petrology of gabbroic rocks from the Mid-Cayman Rise spreading Center. *J. Geophys. Res.*, 92:658-682.
- Engel, C. G., and Fisher, R. L., 1975. Granitic to ultramafic rock complexes of the Indian ocean ridge system, western Indian ocean. *Geol. Soc. Am. Bull.*, 86:1553-1578.

- Ernewein, M., Pflumio, C., and Whitechurch, H., 1988. The death of an accretion zone as evidenced by the magmatic history of the Sumail ophiolite (Oman). *Tectonophysics*, 151:247–274.
- Fisher, R. L., Dick, H.J.B., Natland, J. H., and Meyer, P. S., 1986. Mafic/ultramafic suites of the slowly spreading Southwest Indian Ridge: PROTEA Exploration of the Antarctic plate boundary, 24°E–47°E. *Ophioliti*, 11:147–178.
- Fisher, R. L., and Sclater, J. G., 1983. Tectonic evolution of the Southwest Indian Ocean since the Mid-Cretaceous: plate motions and stability of the pole of the Antarctica/Africa for at least 80 Myr. *Geophys. J. R. Astron. Soc.*, 73:553–576.
- Fornari, D. J., Perfit, M. R., Malahoff, A., and Embley, R., 1983. Geochemical studies of abyssal lavas recovered by DSRV Alvin from eastern Galapagos Rift, Inca Transform, and Ecuador Rift. 1. Major element variations in natural glasses and spatial distribution of lavas. *J. Geophys. Res.*, 88:10519–10529.
- Fox, P. J., and Stroup, J. B., 1981. The plutonic foundation of the oceanic crust. In C. Emiliani (Ed.), *The Oceanic Lithosphere (The Sea, v. 7)*: New York (Wiley), 119–218.
- Hebert, R., Bideau, D., and Hekenian, R., 1983. Ultramafic and mafic rocks from the Garret Transform Fault near 13°30'S on the East Pacific Rise: igneous petrology. *Earth Planet. Sci. Lett.*, 65:107–125.
- Juster, T. C., Grove, T. L., and Perfit, M. R., 1989. Experimental constraints on the generation of FeTi basalts, andesites and thiodacites at the Galapagos Spreading Center, 85°W and 95°W. *J. Geophys. Res.*, 94:9251–9274.
- Juteau, T., Ernewein, M., Reuber, I., Whitechurch, H., and Dahl, R., 1988. Duality of magmatism in the plutonic sequence of the Sumail Nappe, Oman. *Tectonophysics*, 151:107–135.
- Kirkpatrick, R. J., 1977. Nucleation and growth of plagioclase, Makaopuhi and Alae lava lakes, Kilauea Volcano, Hawaii. *Geol. Soc. Am. Bull.*, 88:78–84.
- Langmuir, C. H., 1989. In-situ fractional crystallization. *Nature*, 342:512–515.
- Marsh, B. D., 1988. Crystal capture, sorting, and retention in connecting magma. *Geol. Soc. Am. Bull.*, 100:1720–1737.
- McBirney, A. R., and Noyes, R. M., 1979. Crystallization and layering of the Skaergaard intrusion. *J. Petrol.*, 20:591–624.
- Meyer, P. S., Dick, H.J.B., and Thompson, G., 1989. Cumulate gabbros from the Southwest Indian Ridge, 54°S–7°16'E: implications for magmatic processes at a slow spreading ridge. *Contrib. Mineral. Petrol.*, 103:44–63.
- Miyashiro, A., and Shido, F., 1980. Differentiation of gabbros in the Mid-Atlantic Ridge near 24°N. *Geochem. J.*, 14:145–154.
- Naslund, H. R., 1976. Mineralogical variations in the upper part of the Skaergaard intrusion, East Greenland. *Year Book, Carnegie Inst. Wash.*, 75:640–644.
- Perfit, M. R., and Fornari, D. J., 1983. Geochemical studies of abyssal lavas recovered by DSRV Alvin from eastern Galapagos Rift, Inca Transform, and Ecuador Rift. 2. Phase chemistry and crystallization history. *J. Geophys. Res.*, 88:10539–10550.
- Robinson, P. T., Von Herzen, R., et al., 1989. *Proc. ODP, Init. Repts.*, 118: College Station TX U.S.A. (Ocean Drilling Program).
- Serri, G., 1980. Chemistry and petrology of gabbroic complexes from the northern Apennine ophiolites. In Panayiotou, A. (Ed.), *Proc., Int. Ophiolite Symp.: Cyprus (Cyprus Geol. Surv.)*, 261–272.
- Streckeisen, A., 1976. To each plutonic rock its proper name. *Earth Sci. Rev.*, 12:1–33.
- Tiezzi, L. J., and Scott, R. B., 1980. Crystal fractionation in a cumulate gabbro, Mid-Atlantic Ridge. *J. Geophys. Res.*, 85:5438–5454.
- Wager, L. R., and Brown, G. M., 1967. *Layered Igneous Rocks*: San Francisco (Freeman).
- Walker, D., Shibata, T., and DeLong, S. E., 1979. Abyssal tholeiites from the Oceanographer Fracture Zone. II. phase equilibria and mixing. *Contrib. Mineral. Petrol.*, 70:111–125.
- Walker, D., and DeLong, S. E., 1984. A small Soret effect in spreading center gabbros. *Contrib. Mineral. Petrol.*, 85:203–208.

Date of initial receipt: 17 October 1989

Date of acceptance: 26 June 1990

Ms 118B-136

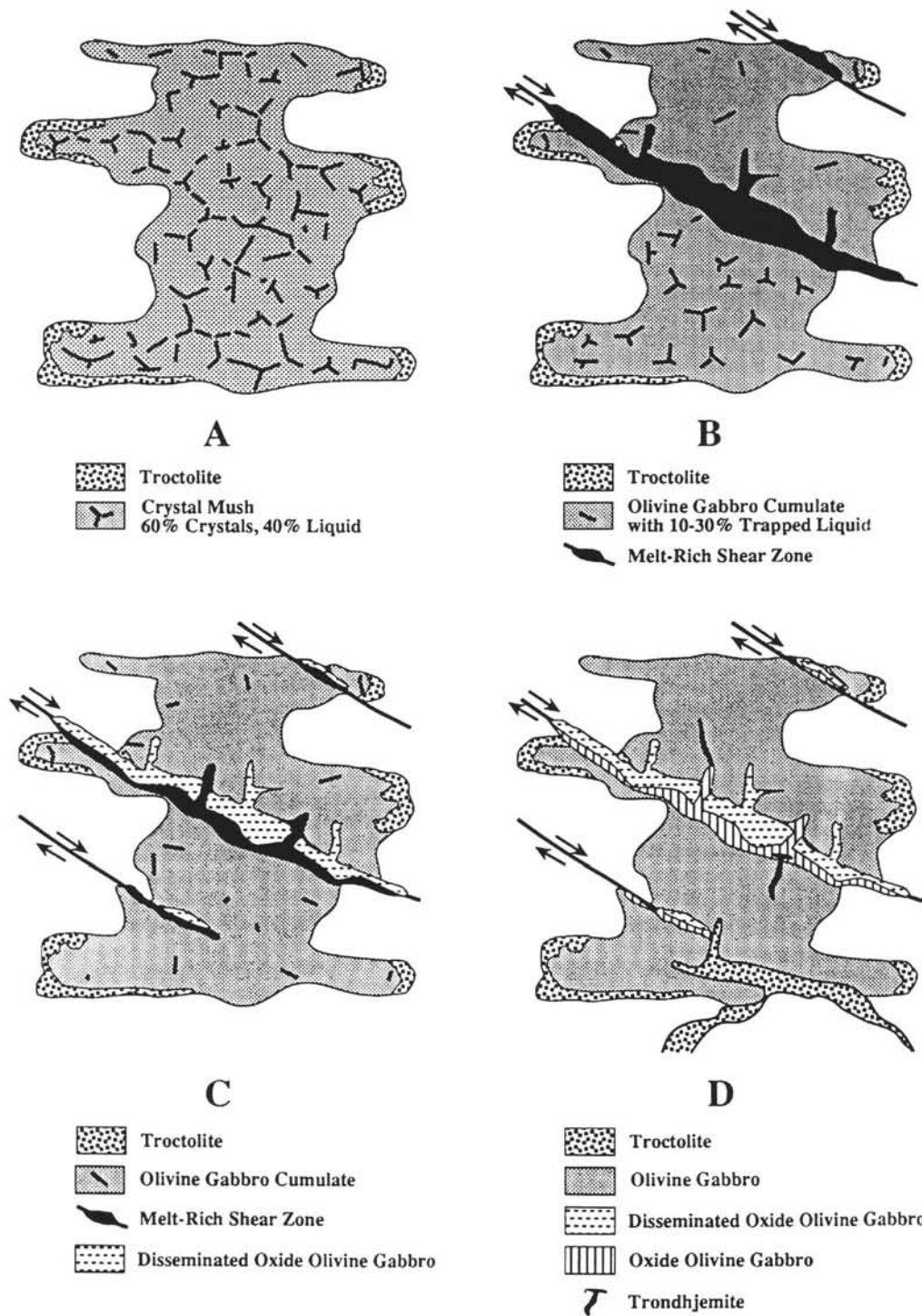
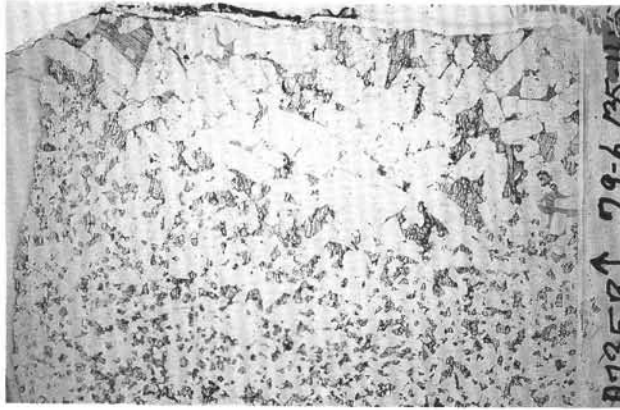
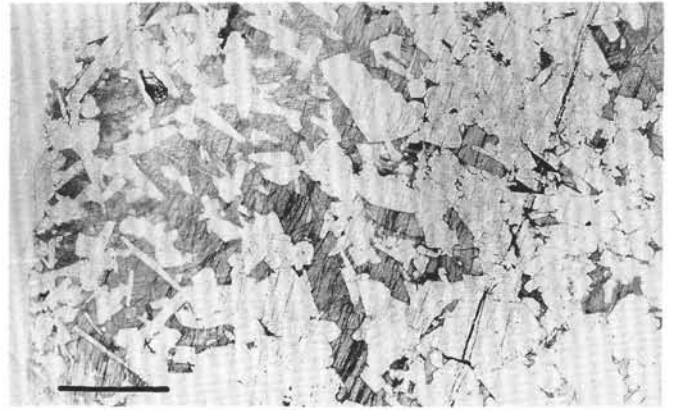


Figure 12. A schematic model for the crystallization of gabbros at Hole 735B. Cooling of an irregularly shaped magma chamber results in the crystallization of troctolitic cumulates on the margins and the formation of a crystal mush with approximately 60% crystals (10% OL, 57% PLAG, and 33% CPX) and 40% melt. Frame A (upper left), until this stage, thermal and compositional convection through the cumulate pile have kept most of the crystals in equilibrium with the melt. Continued crystallization, however, begins to close melt channels sealing off pockets of residual melt and promoting fractional crystallization. This leads to the generation of evolved melts in isolated pockets. As the residual porosity is reduced, the rigidity of the crystal pile increases to a point where shear strain is supported. At this stage, stresses associated with rifting and faulting begin to deform the cumulate pile which is still a crystal mush composed of 20% to 40% liquid. Deformation leads to a channelling of evolved intercumulus melts out of the olivine gabbro cumulate into shear zones (Frame B—upper right). Since the cumulate pile likely cools progressively from the top down, shear zones may migrate with time to deeper levels. In Frame B, two shear zones have drained much of the melt from the upper part of the olivine gabbro cumulate leaving behind 10% residual trapped melt whereas the lower part of the cumulate section still contains approximately 30% melt. Frame C (lower left) depicts the development of a third shear zone and the draining of the lower part of the olivine gabbro cumulate. Crystallization of the evolved melt focused along shear zones proceeds from the top downward, producing first, disseminated oxide olivine gabbros with well-developed igneous lamination, followed by more evolved oxide olivine gabbros (Frame D—lower right). Extension fractures perpendicular to the shear zones are also filled with the evolved gabbros. Extreme fractionation in localized areas leads to the generation of silica-rich melts (trondhjemites) that form veins in the earlier gabbros (Frame D). Frame D also shows troctolites associated with a second intrusion that crosscuts the lower olivine gabbros and oxide gabbros of the first intrusion.



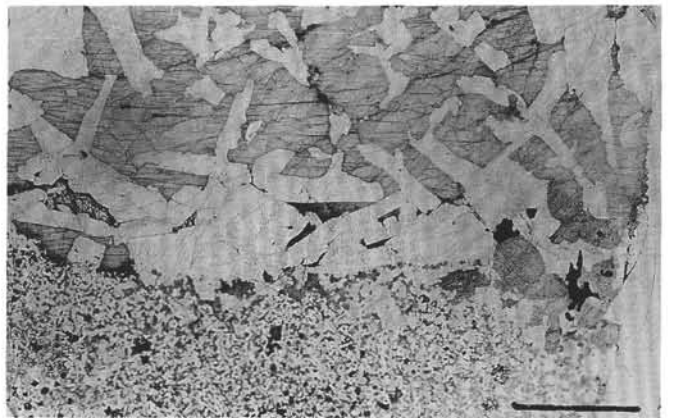
a



b

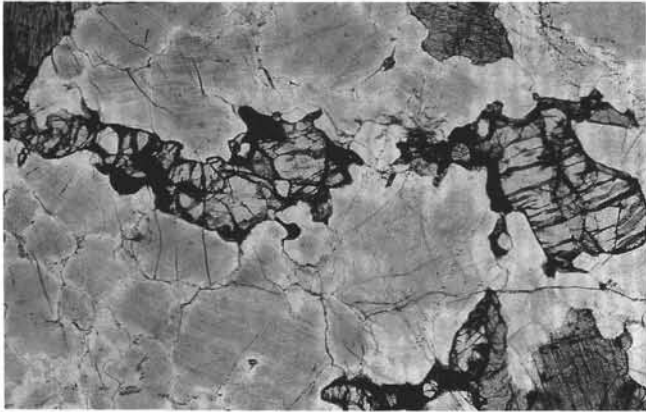


c



d

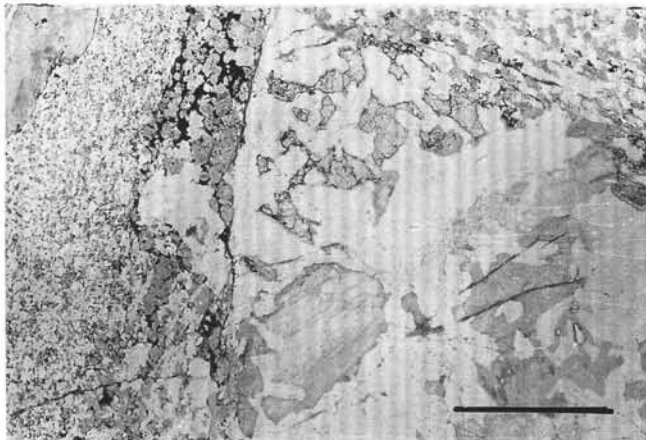
Plate 1. Photomicrographs of representative textures in igneous rocks. a. Sample 118-735B-79R-6, 135–138 cm; coarse-to-fine troctolite with euhedral PLAG, granular OL, and intergranular CPX. Section is 5 cm long. b. Sample 118-735B-85R-8, 39–48 cm; olivine gabbro with ophitic, diopsidic CPX. Note the small size of PLAG chadacrysts, relative to PLAG in the rest of the sample. Section is 3 cm long. c. Sample 118-735B-25R-7, 104–111 cm, olivine gabbro with ophitic to subophitic CPX and granular OL. Section is 5 cm long. d. Sample 118-735B-74X-6, 59–65 cm; oxide microgabbro intruding a coarse olivine gabbro with a large poikilitic CPX. Section is 5 cm long. e. Sample 118-735B-40R-5, 4–5 cm.; OL intergranular to PLAG in a disseminated oxide olivine gabbro. Oxides are commonly developed adjacent to these intergranular OL. Field of view is 3 mm long. f. Sample 118-735B-40R-4, 75–85 cm; disseminated oxide olivine gabbro with a prominent foliation. Section is 2 cm long. g. Sample 118-735B-37X-3, 95–101 cm; olivine gabbro clast (wedge in lower left) in finer-grained disseminated oxide olivine gabbro and oxide gabbro (upper part and lower right). OL along the margin of the clast is equilibrated to more fayalitic compositions than OL in the interior of the clast. Note the CPX xenocryst in the disseminated oxide olivine gabbro at the top of the photo. Section is 5 cm long. h. Sample 118-735B-46R-3, 37–44 cm; coarse-to-fine transition in an oxide olivine gabbro. Section is 5 cm long. This sample shows a preferred orientation of PLAG grains.



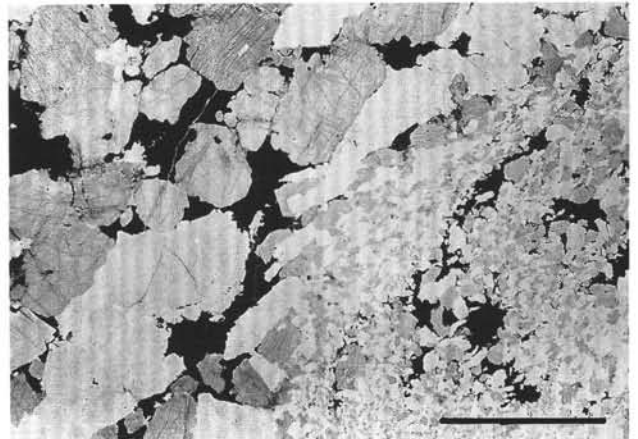
e



f



g



h

Plate 1 (continued).